Journal of Geosciences and Geomatics, 2017, Vol. 5, No. 3, 136-146
Available online at http://pubs.sciepub.com/jgg/5/3/5

DOI:10.12691/jgg-5-3-5

Uranium Mineralization in Gubrunde Horst, Upper Benue Trough, North-East, Nigeria

A.I. Haruna, D.P Ameh*, A. A Mohammed, U.S. Umar

Department of Applied Geology, Abubakar Tafawa Balewa University, Bauchi Nigeria
*Corresponding author: ampitt87@yahoo.com

Abstract The aim of this work is to undertake a study on the occurrence of uranium bearing rocks in the area and infer the source, mechanism of migration and structures or rock type hosting uranium mineralization. This was achieved by an integration of radiation point count, petrographic studies and structural analysis. This is necessary because the Gubrunde uranium occurrence is one of the several known trace to extensive mineralization in North East Nigeria that have been least studied even in the midst of the increasing quest for clean and cheap energy. Moreso, the occurrence of uranium in the area is suspected to be associated with several health implications to the human population. The area has favorable geological environment and conditions for uranium mineralization. Field relationship shows that structurally and tectonically controlled Cretaceous continental sandstones are underlain by acidic granites of the Precambrian basement complex. These are in some places, intruded by much younger volcanic which forms traps for uraniferous solution being transported by hydrothermal fluid in structural conduits. Structural analysis of structures in the area showed a NNE-SSW deformational trend. Samples of rocks from the entire area shows dark to brown opaque minerals suspected to be uranium (Uraninite or Coffinite). Radiation point count confirms the occurrence of radiation ranging from 7.5×10^4 µCi - 6.40×10^5 µCi concentration levels. There is structural and geochemical control to mineralization in the area. Radiation levels at some points were noted to be above human tolerable levels.

Keywords: *Coffinite, deformation, Gubrunde. mineralization, radiation, silicification, uraninite*

Cite This Article: A.I. Haruna, D.P Ameh, A. A Mohammed, and U.S. Umar, "Uranium Mineralization in Gubrunde Horst, Upper Benue Trough, North-East, Nigeria." *Journal of Geosciences and Geomatics*, vol. 5, no. 3 (2017): 136-146. doi: 10.12691/jgg-5-3-5.

1. Introduction

The world total requirement for uranium until the end of this century has been estimated at several million tons (OPEC 1970). The energy crises occasioned by the oil windfall, expanding industrialization and the search for clean alternative source of energy is making the search for uranium as a viable source of clean alternative energy worthwhile. Sustainable uranium exploitation all over the world is a huge challenge to all stakeholders. This scenario has resulted in increase awareness for uranium. Uranium is expected to top the demand due to its peculiar nuclear properties.

Presently, over 90% of the western world's low cost reserves extractable at profit are in Australia, Canada, France, some Africa nations and the USA. It is expected that these countries may run out of reserve in the nearest future. It is therefore necessary that uranium exploration and development commences in other nations with geologically favorable environment so as to find new reserve.

Nigeria as a developing nation has a vast spread of Geological environment and conditions favorable for uranium mineralization. Though uranium deposits are known to occur in many parts of the world and in varied sections of the earth's crust, they are found in well-defined provinces, mainly Precambrian terrain in continental sediments derived from uraniferous older rocks and in association with acid igneous rocks [7]. Uranium as a lithophile element is widely distributed in granites, arkosic sediments, black shale and sea water.

Gubrunde horst has all the geological environment necessary for uranium mineralization; Precambrian basement terrain and continental sediments derived from uraniferous older rocks in association with acid igneous rocks with deformational structures [2,7,8,12]. Infact, uranium occurrence in the area has been reported by [4,17]. Also, there has been reports of radiation and elevated uranium concentration in groundwater in the area [3]. This is thought of to have originated from the mineralized uranium source rock. This might pose health hazards including cancer and kidney problems as a result of ionizing radiation from uranium in groundwater due to chemical toxicity of uranium isotopes [5]. This research evaluates the occurrence of uranium mineralization in the area by an integration of structural, radiation count and petrographic methods and seeks to create awareness on the health implications of the eminent contamination and radiation from uranium.

2. Literature Review

Reference [2] in their Na-metasomatism and uranium mineralization studies of Kitongo Northern Cameroon, observed that the Kitongo uranium occurrence is hosted by granitic rocks that include interleaved sequences of metasedimentary and metavolcanic rocks, collectively termed Poli Group. Uranium mineralization and Na-metasomatism were seen to be related and structurally controlled. The most promising uraniferous bodies in the area are intimately related to intersections between the ductile ENE-trending faults and the brittle conjugate R' faults postdating the shearing event. According to them, the concentration of uranium at fault intersections rather than along individual faults suggests that these zones that are dilatational in nature were also highly permeable and therefore the hydrothermal fluids ponded there could readily precipitate U therein. The host granite and associated granodioritic rocks in the area are weakly metaluminous, peralkaline, and are calc-alkaline. Using data from years of multidisciplinary geological research, [13] ascertained one deposit and four occurrences of uranium minerals in permo-Triassic sedimentary rocks in eastern Serbia. The minerals were the fissure-filling type and exogenic because they are mostly epigene in nature. Relevant geological information were used to derive a genetic model of uranium mineralization in the Permo-Triassic sedimentary rocks of the Stara Planina. A geochemical barrier zone was identified in the sedimentary rocks that contained uranium mineral ore. This geochemical barrier area included crescent-shaped, flat-lens, or vein-like ore bodies. Reference [12] used X-ray absorption fine structure analysis to confirm the reduced valence state of uranium and in combination with high-resolution electron microscopy and electron probe microanalysis, the mineral was identified as Coffinite ($USiO_4$). In their study, a strong positive correlation between the sizes of the Coffinite crystals and their surrounding carbonized rings revealed that the Coffinite is authigenic, and its crystallization-produced radiation resulting in the radiolysis of surrounding organic matter. The association of various biogenic metal sulfides, phosphates, and abundant organic substances within the Ni-Mo sulfide-enriched ore suggests that biological adsorption may have participated in the enrichment of soluble U and that microbial sulfate reduction might have facilitated the uranium mineralization. Reference [15] observed an appearance of quartzite due to intense silicification in the sheared basement and overlying rocks of Delhi. Grab samples collected from the shear zone rock analyzed up to 93ppm U_3O_8 and <10ppm ThO_2, this was reported to be anomalous compared to unsheared rock which analyzed 51ppm eU_3O_8, up to 5ppm U_3O_8 and 80ppm ThO_2. Gamma-ray logging of boreholes drilled by GSI across this shear zone indicated uranium mineralization of the order of 0.030% eU_3O_8 x 5.40m and the primary radioactive mineral was identified as Uraninite [11]. identified two-mica leucogranite and muscovite pegmatitic granite as the most favorable host rocks for uranium and thorium mineralization. The muscovite pegmatitic granite shows evidence of post-magmatic alteration whereas the two-mica leucogranite were regarded as fresh. The origin of these minerals was explained to be mainly related to alteration of primary minerals by the action of oxidizing fluids, mobilization of uranium and then re-deposition in other forms. Redistribution by circulating meteoric waters might have taken place. Reference [9] posted that U and Th contents of granitic rocks generally increase during differentiation, although in some cases they decrease. The Th/U ratio can either increase or decrease, depending on redox conditions, the volatile content or alteration by endogene or supergene solutions. Uraniferous rhyolitic vein occupying fracture (N80°E-S80°W) within the eastern margin of singhora rocks in Jabu village was reported by [16] to contain granitic composition. This was confirmed by thin section studies. Presences of phenocrysts of bipyramidal quartz, euhedral senidine and biotite in fine grained glassy to devitrified groundmass was used to classified the rock to rhyolitic category. The rhyolitic vein analyzed uranium (28 to 100 ppm) associated with limonite, goethite and apatite. This Uranium bearing rhyolitic vein was fracture filled in the basement rocks and has significance in the light of uranium-sulphide mineralization. Reference [10] reported uranium mineralization along the unconformity contact between the basement granites and the overlying Chandrapur sediments of the Chhattisgarh Supergroup. A number of uranium occurrences, spread over an area of 20 km^2 were delineated with surface samples analyzing up to 0.39%U_3O_8 in sediments, 2.72%U_3O_8 in basement granites and up to 0.21 %U_3O_8 in basic dykes. The uranium mineralization is confined to the basement granites and the overlying sediments proximal to the unconformity contact. The basic dykes traversing the basement granites were also mineralized. QAP plots of basement granites fall in the field of syeno- to monzo-granites. The granites are highly altered (chloritised, kaolinised and ferruginized) particularly near the unconformity contact. In their structural and mineral alteration study of Zona uranium anomaly, Reference [18] summarized that the Zona U anomaly is a sandstone-hosted anomaly which is structurally controlled. Three main zones of mineral alteration were recognized as; silicified zone; a red-brown ferruginized (hematite) zone and a brownish/yellowish-brown ferruginized (goethite) zone. These zones are identifiable by brecciation and kaolinitisation. The U mineralization is epigenetic in origin and post-dates the main tectonic deformations. Uranium was leached from the Basement Complex granites and at same time disseminated in the sandstones. Percolating groundwater subsequently concentrated the ore followed by the formation of kaolinite and goethite at low temperatures. The main U mineral is autinite. Reference [19] reported that mineralization in Kanawa violaine is associated with pervasive silicification and phyllosilicate alteration of the feldspar phases. The uranium mineralization occurs as Uraninite-rich veinlets within brittle structures. Feldspars in phenocryst were most affected by alteration during the brittle-ductile deformation of the host rock. Plagioclase was extensively altered to micas, chlorite ± epidote, ±albite. Alkali-feldspar deformed mainly by transgranular fracturing as a result of shearing to yield clasts with lensoid shape. Quartz shows little evidence of brittle deformation but extensive in situ recrystallization. The hydrothermal fluid remobilized and subsequently concentrated the uranium. This fluid was enriched in Si4+, Na+ and K+, possibly derived from plagioclase alteration. This lead to association of the ore with phyllosilicate and

silicification alterations. Reference [4] observed that the Wuyo-Gubrunde Horst in the northeastern Nigeria consists of migmatites gneiss, unaltered, altered, and sheared porphyritic granites, pegmatites, aplites, basalts, and sandstone. Uranium was reported in rhyolite, sheared rocks, and sandstone within the area. The petrogenesis of the granitoid and associated rocks in the area was evaluated in the light of new geochemical data, evaluation of the petrogenesis of the granitoid using geochemical data showed that the U content of altered porphyritic granite is highest and hydrothermal-related. They opined that the U occurrence in the Wuyo-Gubrunde Horst is believed to be sourced from the adjoining Bima sandstone in the Benue Trough, which locally contains carbonaceous zones with anomalously high concentrations of U. The Fe2+/Fe3+ redox fronts formed by alteration of the iron-rich basalts provided the requisite geochemical barrier for U-bearing hydrothermal fluid, causing enrichment of U leached and mobilized from the sandstone through fractures in the rocks. Of uranium occurrences in the northeast of Nigeria. Reference [17] maintained that they uranium mineralization in the northeast of Nigeria are sandstone-hosted and vein-type mineralization. Sandstone-hosted deposits occurs in sedimentary/ volcanosedimentary sequences and structurally controlled at Zona and Dali, while the vein-type mineralization occurs in the deformed migmatites and granitoid at Gubrunde, Kanawa, Ghumchi, Mika and Monkin-Maza deposits.

This present research will evaluate the occurrence of uranium mineralization in the area by an integration of structural, radiation count and petrographic methods and seeks to create awareness on the health implications of the eminent contamination and radiation from uranium.

3. Geological Setting

The area is accessible by the major Biu-Dadinkowa road. Access to the area is by footpaths and cattle tracts. The area is located within longitude E11^{0}42$^{'}$44.0'' to E11^{0}41'20.7'' to latitude N10^{0}22'05.8''and N10^{0}23'34.5'' as shown in Figure 1. Gubrunde horst is bounded to the north by the low lying Bryel Graben and to the south by the low lying Zange Graben which is overlain by the Cretaceous Bima Sandstone [7]. The Gubrunde horst block originated by tectonic uplift of the basement rock between NE-SW trending faults. It is made up of mostly Granitic rocks associated with Rhyolite veins and brecciated Granite [7]. The area is underlain by crystalline basement rock of Precambrian age. The Horst itself and the associated graben were produced in the Albian after being subjected to metamorphism, granitization and tectonism. The basement rock type in the area include migmatites, gneisses, diorite and granodiorite, fine grained granites and syn-tectonic granites consisting of porphyritic and equigranular grains. Essential minerals of the area are microcline, plagioclase, orthoclase, quartz and micas. Fractures abound in the area, the most significant is the NE-SW fault that produced the horst. The mineralized zones are located along N-S trending shear zone which extends more than 4km and has rhyolitic peaks along the margin [8]. The mineralized zone shows intense alteration and brecciation. Ore minerals identified are phosphor-uranylite, meta-autinite and kasonites along with traces of Galena and chalcopyrite [8]. The mineralize rhyolite contain appreciable quantity of apatite, glass and Fe-Ti oxides which are highly remobilized [8].

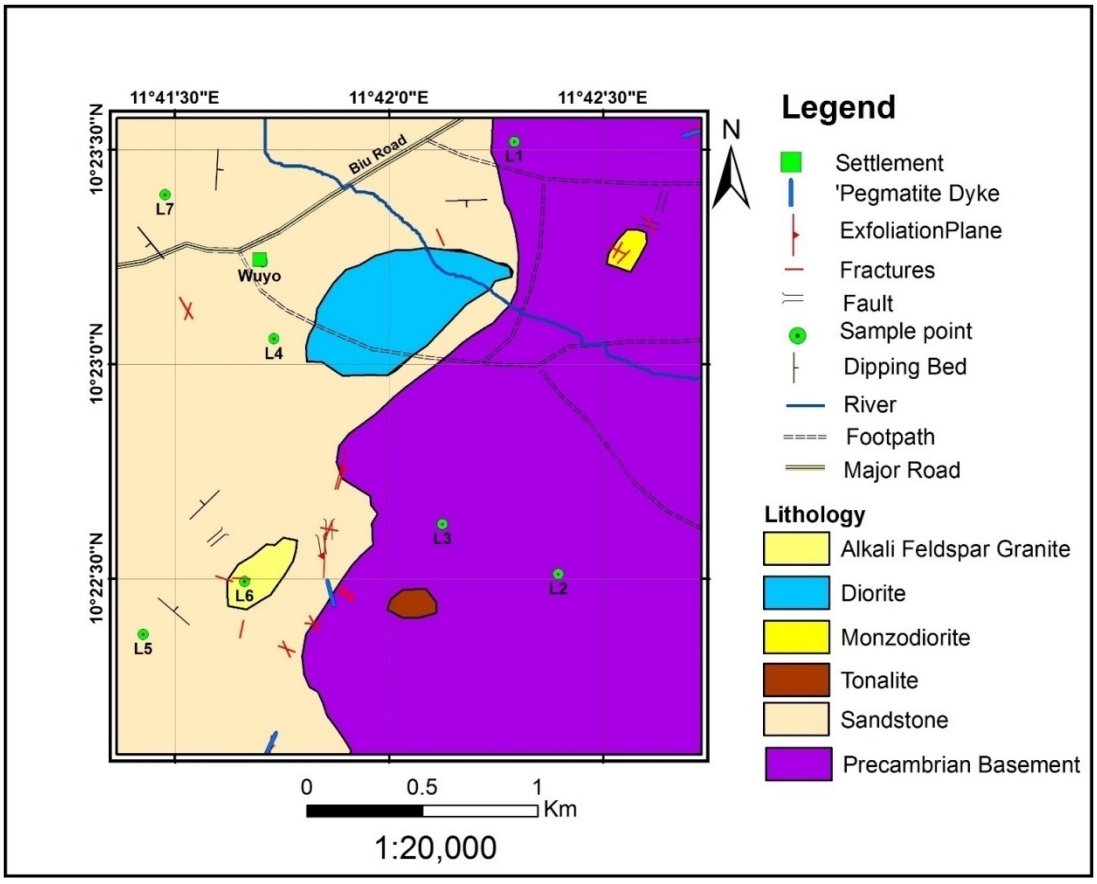

Figure 1. Geologic map of the area

4. Methodology

Geologic reconnaissance was conducted around the area to determine the field relationship between the rock types. The entire Gubrunde horst was traversed. Positions of structures and lithologic changes were noted and was used to produce the geologic map (Figure 1). Samples were collected systematically at selected points for laboratory radiation point count [14,15]. The attitudes of major structures such as fractures, faults and exfoliation planes were measured and recorded. The attitudes of geologic structures measured in the field were plotted to a rose diagram (Figure 2) using Roxeta software. This was done to show the direction of the structures so as to have an idea of the paleo-deformational forces. Petrographic studies was done by examining thin sections of the rocks with petrographic microscope under both cross and plane polarization [14]. This was to see the minerals contained in the rock. This will help ascertain the presence of uranium minerals. The photomicrographs are presented as Figure 4 – Figure 10. Representative samples were collected across the study area, the samples collected were exposed to Geiger-muller counter for radiation counting. Geiger-muller counter consist of a processing unit and the detector. The detector was clamped close to the sample and the total radiation detected was processed and displayed digitally. Radiation counting was induced by a radiation source kept under the sample and thereafter, the value of the radiation source was subtracted from the total count displayed on the counter. The radiation count is for the total radiation (alpha, beta and gamma). This was done to have an estimate of the concentration or intensity of radiation from the sample. This will be helpful in classifying the area into concentration zones as well as help in advising for health implication.

5. Result and Discussion

5.1. Structural Analysis

Field data such as attitude of fractures, fault, dykes, ridge, and exfoliation planes were treated to structural analysis using the Roxetta. Rose plot showed that most deformational structure trend in the NNE-SSW direction. (Figure 2). This is in line with the Pan-African deformational belt. A more detailed look at Figure 2 show that some deformational structure fall in the NEE-NWW direction which could be interpreted to mean the aftershocks or ripple effect of the NNE-SSW major deformational trend. A reconnaissance traverse of the entire Gubrunde horst revealed that the horst is surrounded by ferruginized and silicified Bima sandstones with blocks of basement rocks ranging from Granites, Gneisses, Diorites, Tonalites and Monzodiorite towards the peak region agreeing with the rock types listed by [6]. Rock units host several deformational structures such as faults, fractures, shear zones, pegmatitic and granitic intrusion and exfoliation planes.

Overall observation in the area suggests a long period of tectonic deformational activity starting from the Precambrian to the mid-Santonian. The mid-Santonian episode of the tectonic deformation is thought to result in the structures hosting uranium in the area. The structures and age of the structures of the area is comparable to the structures and age of uranium prolific areas in Niger-Republic. The structures and lithology are the same geologic environment necessary for mineralization as seen from the model of other uranium producing areas. Precambrian basement terrain and continental sediments derived from uraniferous older rocks and in association with acid igneous rocks with deformational structures [7,8]. The basement rocks are the oldest in age, emplaced during the Precambrian times [8]. The basement rocks include Granites, Gneisses, Migmatites and Diorites. They are the rocks of the Migmatites-Gneiss complex (MGC) intruded by younger granites followed by deformation accompanying intrusive activity. The basement rocks were worked on by agents of denudation following the continental (fluvial) condition of the environment. This resulted in the deposition of Bima Sandstone. The Mid-Santonian episode of tectonic activity provided a reworking of both the basement and sedimentary rocks in the area. The faults and fractures formed in the Precambrian were rejuvenated by this tectonic episode while also forming new deformational trends on the basement and sedimentary rocks. These new deformational structures are in same direction as the Pan-African deformation and are deep seated. The faults and accompanying structures (shear and Fractures) act as major conduits to passage of hydrothermal fluids and remobilized groundwater that contain uranium ore and hence mineralized the proximate sandstones and basement areas [2]. The passage of this fluid resulted in large scale silicification of the sandstone and other rocks especially in areas around the fault zones. Silicification (also reported by [15]) is the predominant alteration type in the area and can be taken as the chemical pathfinder to uranium mineralization in the area.

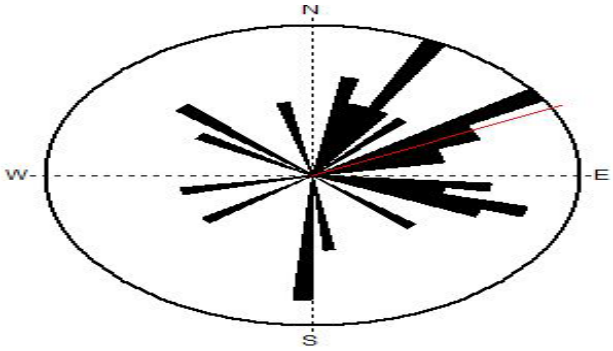

Figure 2. Rose Diagram showing the direction of deformational structures

5.2. Laboratory Radiation Count

Representative samples collected from the field were subjected to radiation count using the Geiger-Muller counter. Radiation counting was induced by a radiation source placed under the sample and thereafter, the value of the radiation source was subtracted from the total count. The result is presented as the geochemical map (Figure 3). The radiation count data was used to arbitrarily divide the area into three geochemical zones.

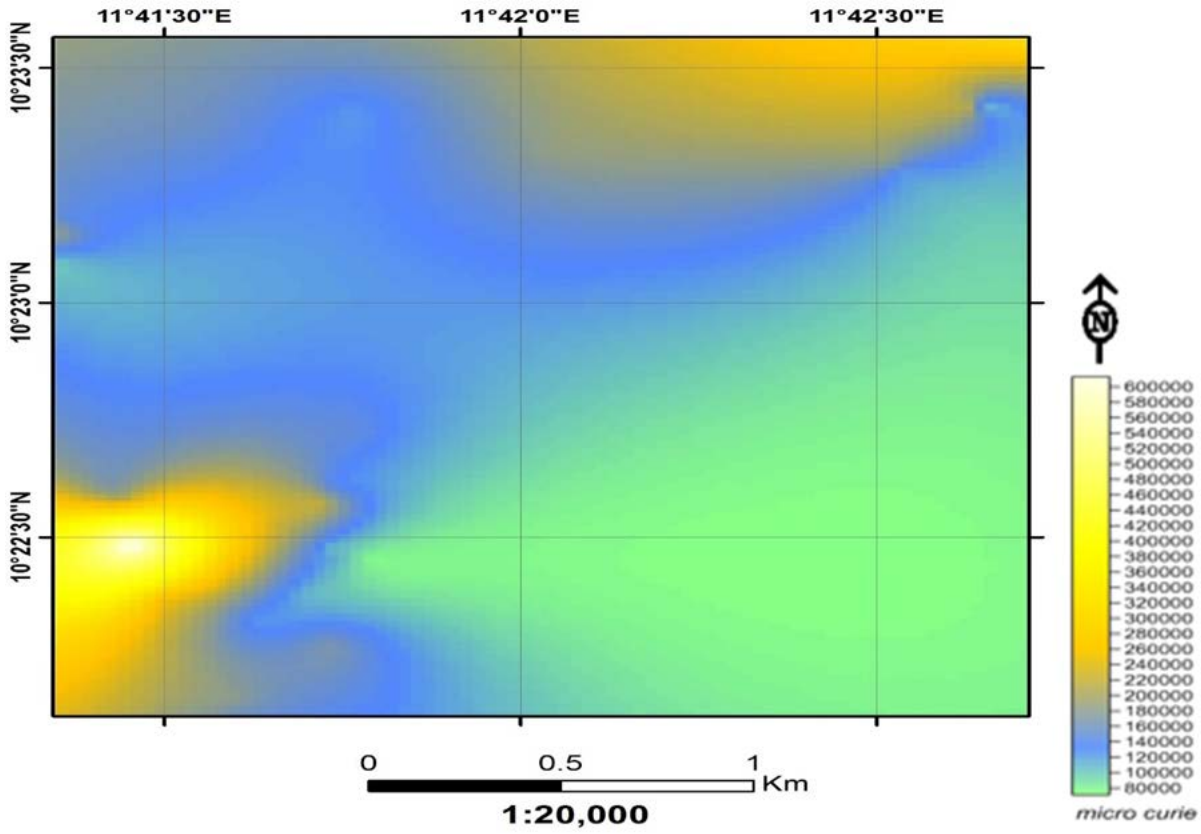

Figure 3. Geochemical map showing concentration of Uranium in Gubrunde Horst

1. The anomalously low Areas: Areas with radiation count concentration of (7.5×10^4-9.9×10^4) µCi, they are the green areas in the geochemical map. This area corresponds to areas with less surface deformation (faults and fractures) as a result, the uranium were not connected to and mobilized into this area (Figure 3).
2. The background Areas: These are areas with radiation count concentration between (1.0×10^5-$2.0\times10)^5$ µCi. They are the blue areas in the geochemical map. Over 60% of the study area has the background concentration value (the term "normal" as used does not mean it is safe, it is "normal" in comparative sense with the concentration of other mapped areas. It falls within the area with fairly good distribution of deformational structures.
3. The high concentration Areas: These are areas with high (above normal) radiation count concentration of uranium. They have count concentration values of between (2.01×10^5 -6.40×10^5) these areas correspond to areas with younger intrusions, pegmatitic ridge and dykes and deep seated structural deformations. They are generally elevated area favoring mobilization of uranium fluids. They are the yellow areas on the geochemical map (Figure 3). They are generally the elevated areas (peak heights) and are ridged, they have high network of fault, fracture and shear zones and are made up of predominantly silicified sandstones. The high network of faults and fractures and its proximity to the fault line may account for the very high concentration of uranium and its attendant silicification. The uranium deposits here are thought of as secondary in nature because they were mobilized into sandstone compared to the uranium in the pink areas may be a mixture of primary and secondary deposits. Primary in the sense that series of the younger volcanism resulted in uranium mineralization in the basement areas (though few) and secondary in the sense that some sandstones also have remobilized uranium deposits from well-connected and deep seated faults and fractures.

Uranium is a radioactive element and is prone to spontaneous disintegration and emission of radioactive particles. Continuous exposures of the human tissues and cells to these emissions have been known to cause serious bodily damage. According to medical reports, exposure of human cells to radiation dose of up to 25rem/yr. is normal and can be tolerated by the body immune system but exposures beyond this limit is harmful to the body. Harmful effects of excess radiation dose exposures include malignant or cancerous growth of body cells, genetic mutation, severe skin irritation and even death. Emission of radioactive particles can be ingested by humans through drinking of water containing dissolved uranium, consumption of fruits and food grown in uranium containing soil/water and exposures to the disintegrating particles of uranium contained in soil and rocks by any form of contact.

The sample of rocks taken from the area was found to contain uranium count concentration in rems equivalent of between $7.5\text{x}10^4$-$6.4\text{x}10^5$µCi. This may be above the allowable limit of human exposure dose and hence will portend a health danger to the inhabitants because stream and groundwater are the source of water in the area and also, the community is majorly agrarian with most of her food grown locally. It should be noted that the count data supplied is for a representative sample only. Actual

emissions in the area are expected to be in multiples of this value.

5.3. Petrographic Analysis

Petrographic study of rock samples from the area was done to be able to identify uranium minerals in thin section under plane and cross polarization. Seven samples were studied in thin section. Samples of rocks from the entire area shows dark to brown opaque minerals suspected to be uranium (Uraninite or Coffinite). This mineral is opaque, it has no cleavage, high refractive index and relief and parallel yellow to brown extinction (encircled in Figure 4 - Figure 10). Samples L1, L2, L3, L4, L5 and L6 have this suspected uranium mineral. However, sample L6 (Figure 9) showed the highest concentration of the suspected mineral. It is important to note that sample L6 was gotten from the peak of the ridge near the fault plane. This supports the fact that the deformational structures are the conduits for the mineralizing fluid thus mineralization can be said to be structurally controlled in the area. From petrographic study of rock samples, feldspar group of mineral seems to be mutually exclusive in most part of the area because the occurrence of plagioclase group of feldspar in a sample keeps out the alkali feldspar except in a L1 (Figure 4) where they co-exist. Generally, plagioclase group of feldspar predominate the area as also reported by [1]. The area also show good quartz content indicative of intense silicification.

Figure 4. Photomicrograph of L1 (a) under cross polar, b) Under plane polar

Figure 5. Photomicrograph of L2 (a) under cross polar, b) Under plane polar

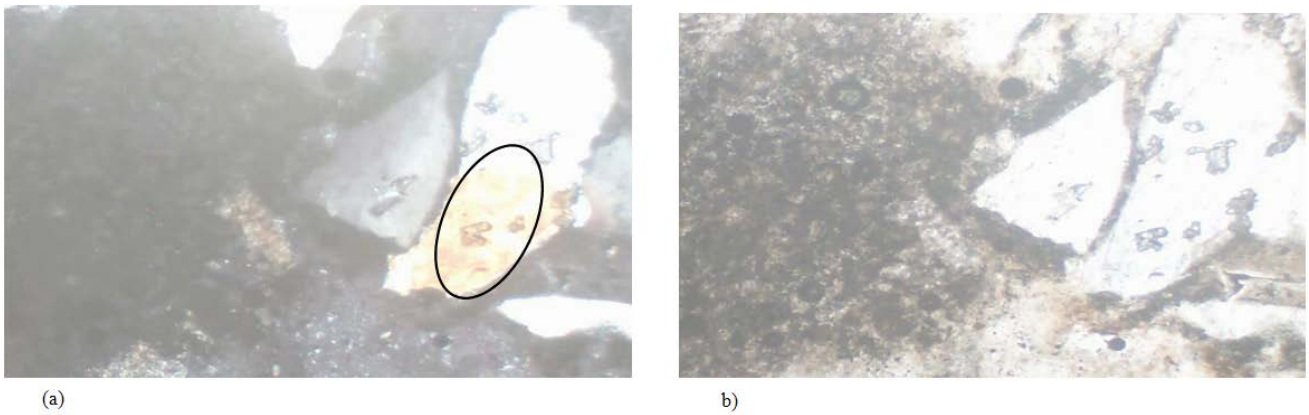

Figure 6. Photomicrograph of L3 (a) under cross polar, b) Under plane polar

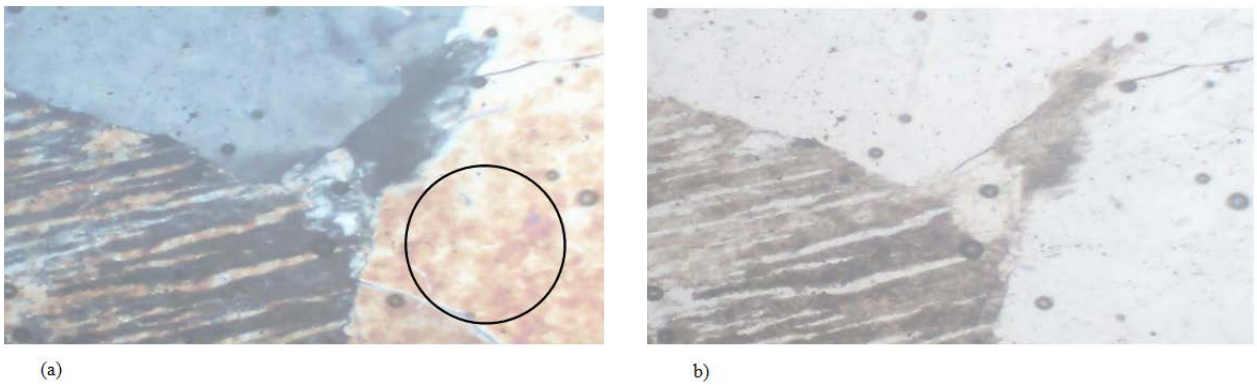

Figure 7. Photomicrograph of L4 (a) under cross polar, b) Under plane polar

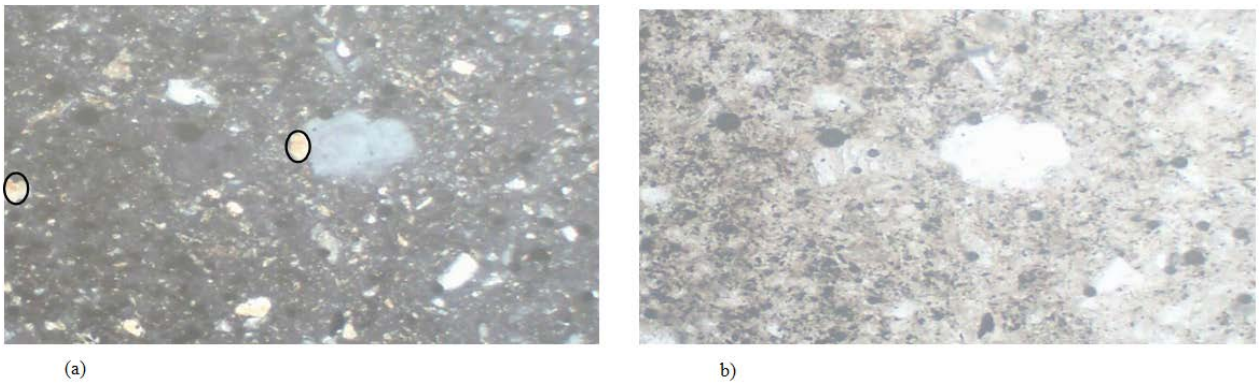

Figure 8. Photomicrograph of L5 (a) under cross polar, b) Under plane polar

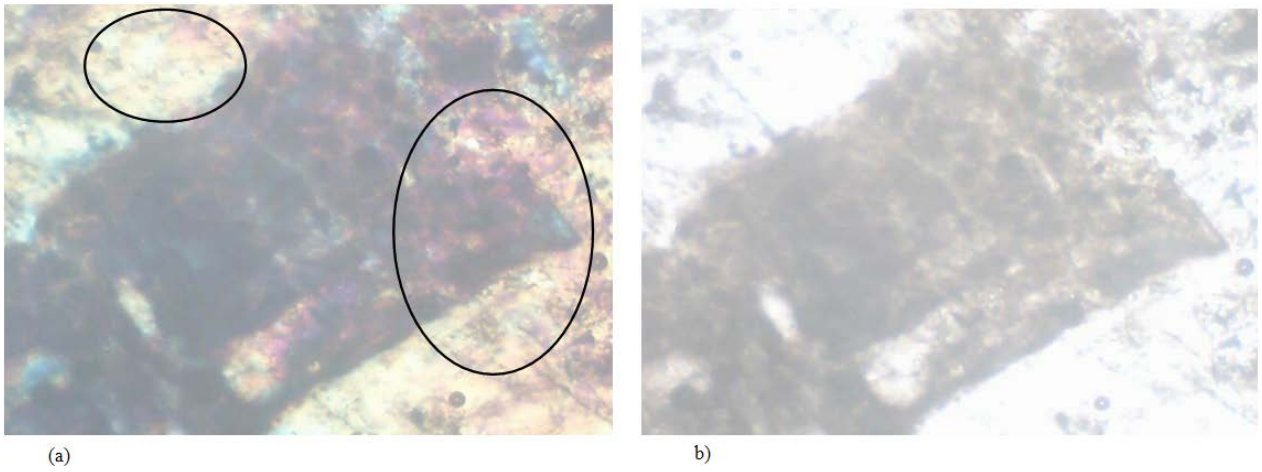

Figure 9. Photomicrograph of L6 (a) under cross polar, b) Under plane polar

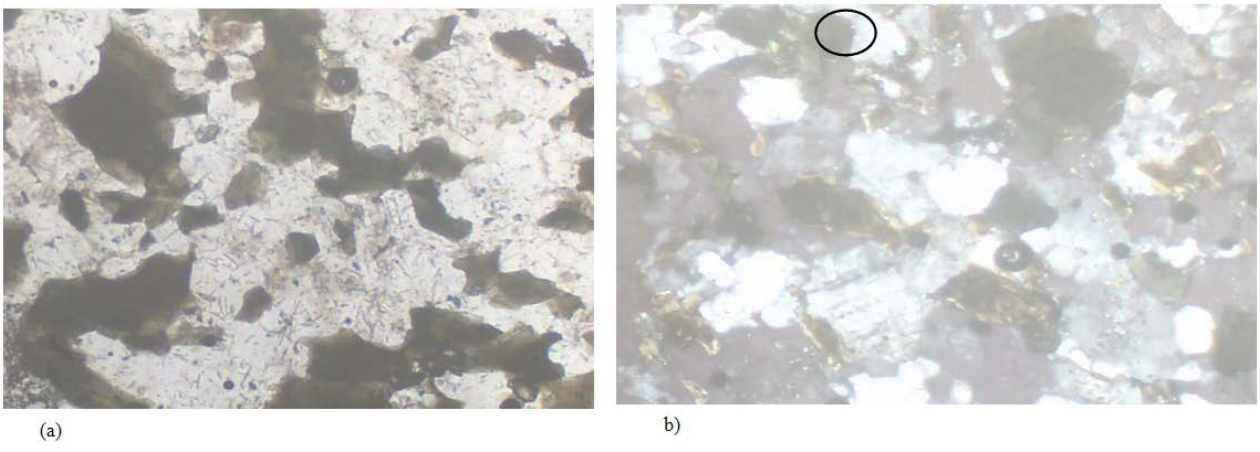

Figure 10. Photomicrograph of L7 (a) under cross polar, b) Under plane polar

Table 1. Table of Radiation Count Values of Samples.

Sample ID	Description	Radiation point count (μCi)
L1	Gneiss	1.85×10^{5}
L2	Gneiss	7.50×10^{4}
L3	Gneiss	1.45×10^{5}
L4	Purple Sandstone	1.55×10^{5}
L5	Ferruginized Sandstone	1.82×10^{5}
L6	Feldspathic Granite	6.40×10^{5}
L7	Silicified Sandstone	1.55×10^{5}

The observation from the petrographic studies correlates strongly with the result of the radiation point count. Areas with high concentration of uranium minerals in the thin section also reported high radiation values as presented in the Table 1. Note that L6 which had the highest distribution of uranium minerals in the thin section also had the highest radiation count value.

6. Conclusion

The structural hosts of uranium in the area are the fault and fractures [1]). The uranium ores found in these structures are primary in nature given that the faults and fractures are deep seated and are connected to the volcanic root that emplaced the rock. The primary source of uranium in the area is magmatic. Magma containing elemental uranium as REE starts partial crystallization and the uranium element is further concentrated in the remaining magma melt. The remaining magma melt finally crystallizes to form rocks rich in uranium ore (primary deposits). Another host of uranium is the Bima sandstones and are secondary in nature. These are the most widespread type of deposit in the area. Secondary uranium is formed by the re-mobilization of uranium in rocks by reducing groundwater through structured conduits into sediments. The sandstones are formed as weathering product of Precambrian basement rocks as a result of severe change in environmental factors. The sandstones are deposited on the basement either insitu or transported. The Jurassic tectonism that resulted in further granitization and deformation also fractured and faulted the pre-existing basement cum sediment and a passage way for mineralizing fluid was created. The uranium contained in remaining magmatic melt mixed with reducing groundwater (hydrothermal fluid) thus passed through the Jurassic aged conduits to mineralize the sandstones. This mode of mineralization was also suggested by [1]. This explains why uranium mineralization is highest at sandstone ridges and appear to decrease away from fault zones in sandstones. Reference [1] also explained the difference in concentration of uranium at Kikongo, Northern Cameroon using this analogy. The flow of residual fluid into the sandstones also resulted in the silicification of sandstone. Silicification had been reported by [19] and necessarily provided the much needed reducing environment for uranium mineralization. The sandstone type deposit of uranium is thought to contain the Coffinite ore because of the widespread alteration. The two types of uranium ore proposed for the area corresponds to the sources explained above. The primary deposits is inferred to contain the Uraninite ore *type* because of its primary and unaltered nature in granitic and other equivalent host rocks and the secondary deposits is inferred to contain the Coffinite ore type because of its altered nature in the sandstone host. There is both structural and geochemical control to the mineralization just as has been reported by [1,4,13,17,18] respectively. The health implication of the radiation from uranium could be adverse. Therefore an expert look into the health effect of the radioactive deposits on the people is highly advised and prompts action taken thereafter.

Acknowledgements

The authors reserve gratitude to the village head and people of Gubrunde village for enabling peace and permit to study the area. Our appreciation also goes to Physics Department of Abubakar Tafawa Balewa University, Bauchi for allowing access to and usage of their Laboratory and Equipment. Friends who accompanied us during the fieldwork are also thanked.

References

[1] Ajay, K., Birua, S.N.S. and Raju, A.R, "Geology and Uranuim mineralization around Ampulli area, Papum- pare district, Akunachal, Predesh, North-East India" *Exploration for research for atomic minerals, EARFAM,* v.18, 2008

[2] Arnaud,P.K., Cheo, E.S., Richard, T.G. and Vincent, N. "Na-metasomatism and Uranium Mineralization during a two- stage Albitization at Kitongo, Northern Cameroon", *Structural and Geochemical International Journal of Geosciences*, v.3, pp. 258-279, 2012.

[3] Arabi, A.S., Funtua, I.I., Dewu, B.B.M., Garba, M.L., Yusuf, I.A., Abafoni, J.D and Garba, I. "Uranium Mobility in groundwater from From uranium Mineralized areas around Gubrunde,Northeast Nigeria". *Journal of Engineering Sciences*, v. 2(8), pp.344-349, 2013.

[4] Anthony, B. and Saleh, I.B. "Petrochemical and Tectogenesis of granitoids in the Wuyo- Gubrunde Horst, N.E Nigeria: Implications for uranium Enrichment". *Natural Resource Research*, v. 25(2), 2015.

[5] Argonne National Laboratory (ANL, 2007), Radiological and channel fact sheets to support health risk Analysis of contaminated areas. ANL environmental services division in collaboration with US. Dept. of energy (DOE). EVS, p.174, 2007.

[6] Dahlkamp, F, J. *Classification of Uranium deposits in mineral deposits.* Berlin. v.13, pp.83-104, 1978.

[7] Funtua I.I., Okujeni, C.D. et. al., "Geology and Genesis of Uranium mineralization in Kanawa and Gubrunde Horst". NE Nigeria. *Journal of Mining and Geology*, v. 29 (2) pp. 8-15, 1993.

[8] Funtua, I.I., Okujeni, C.D. et al., "Exploration And mineralization of uranium" *Journal of Mining and Geology*. v.17(1) pp.1-12, 1988.

[9] Gehad, M.S. "Uranium mineralization in the muscovite-rich granites of the shelatin geochemistry, region, Southeastern Desert, Egypt". *Chinese journal of Geosciences*, 2006.

[10] Gupta, P.K., Rajeevan, R., Mukundan, A.R, Deshpande, M.S.M., Shrivastava, V.K and Yadava, R.S. "Uranium mineralization along the NE margin of Proterozoic Chhattisgarh basin around chitakhol, central India: A petromineralogical Study". *Exploration and research for atomic energy*, 2008.

[11] Ibrahim, M.E., Saleh, G.M., Abd El-Nafaty, H.H, *Uranium mineralization in the two mica Granite of Gabal ribdab area, Southeastern desert, Egypt*. National Centre for Biotechnological Information, v. 55 (6) pp.861-872, 2001.

[12] Jun Xu, San-Yuan Zhu., Tai-Yi Luo., Wen Zhou, and Yi-liang Li, *Uranium mineralization and its Radioactive decay induced carbonization in black Shale-hosted polymetallic sulfide ore layer, southwest China.* Society of economic Geology, 2015.

[13] Jovan, K., Zoran, N, and Petar, P, "Genetic model of uranium mineralization in the permo-Triassic Sediment rocks of the stara Planina eastern Serbia". *Elservier,* v.219 252-261, 2009.

[14] Ogunleye, P.O and Okujeni, C.D, "The geology and geochemistry of Zona uranium occurrence, Upper Benue Trough, NE Nigeria". *Nigerian jour. of mining and geology*, v.40 (2) 1-11, 2004.

[15] Panigrahi, B., Shaji, T.S., Sharma, G.S., Yadev, O.P and Nande, L.K. "Anomalous uranium concentration in Archean basement shear at Dhanbasri basin, Rajasthan" *EARFAM*, v. 18, 2008.

[16] Sinha, D.K and Jain, S.K, "Uraniferous rhyolite Protobasin, Near Juba village, Raipur district, Chhattisgarph". *Exploration and resources for atomic Energy*. v.18, 2008.

[17] Saleh, I.B, "Uranium ore deposits in NE Nigeria: Geology and prospect", *Continental journal of earth Sciences*, v. 8 (1) pp.21-28, 2013.

[18] Suh, E.C., Silas, D., Ajayi, T.R. and Matheis, G. "Integrated structural and mineral alteration study of The zona uranium anomaly, Northeast Nigeria". *Journal of African Earth Sciences*, v.27 (1), pp.129-140, 1998.

[19] Suh, E.C and Silas, D, "Fault rock and differential reactivity of minerals in the Kanawa Violaine Uraniferous vein, NE, Nigeria", *Journal of structural Geology*, v.19 (8), pp.1037-1044, 1997.

[20] Suh, E.C., and Silas, D, Mesostructural and microstructural evidences for a two stage tectono-metallogenic model for Uranium. Nonrenewable resources, v.7 (1), pp.75-83, 1998.

SUPPLEMENTARY DATA

Table X. Table of sample location used for petrographic studies.

Sample ID	Field Description	Location
L1	Gneiss	N10 23 30.0 E 11 42 20
L2	Gneiss	N 10 22 30 E 11 42 25
L3	Gneiss	N 10 22 35 E 11 42 15
L4	Purple Sandstone	N 10 23 01.2 E 11 41 45
L5	Ferruginized Sandstone	N 10 22 15.6 E 11 41 15
L6	Feldspathic Granite	N10 22 30 E11 42 25
L7	Silicified Sandstone	N10 23 20 E11 41 30

Table Y. Attitudes of Geologic Structures

GEOLOGIC STRUCTURE	STRIKE READING	DIP READING.
STREAM CHANNEL	N40S	-
RIDGE	N30E	-
FAULT PLANE	S171E	
PEG. DYKE	S345W	-
FRACTURE	S184W	10NE
FRACTURE	N25E	-
PEG. DYKE	N25E	-
FRACTURE	S112E	-
FRACTURE	S110E	-
FRACTURE	S108E	-
FRACTURE	S183W	30NE
FRACTURE	N20E	
FRACTURE	N28E	
FRACTURE	N28E	
AGATE RIDGE	N300W	-
FRACTURE	S108E	18SE
FRACTURE	N18E	
FRACTURE	S102E	
FAULT PLANE	N180S	
FRACTURE	N58E	
FAULT PLANE	N75E	
FRACTURE	N26E	
FRACTURE	N10E	20NE
FRACTURE	S95E	2NE
FRACTURE	N310W	5NE
FAULT PLANE	S230W	18SE
FRACTURE	N314W	2SE
EXFOLIATION PLANE	S130E	16NE
PEG. DYKE	N74E	-
FRACTURE	N60E	
FRACTURE	N10E	
EXFOLIATION PLANE	S182W	
EXFOLIATION PLANE	S98E	
FRACTURE	N58E	-
FRACTURE	N65E	
FRACTURE	N58E	
FRACTURE	N56E	
FRACTURE	N66E	-
FRACTURE	N61E	
FRACTURE	N58E	14NW
FAULT PLANE	S108E	22NE

Table Z. Result of Total Radiation Count of Representative Sample using the Geiger-Muller Counter.

COORDINATE	INFERRED ROCK TYPE/STRUCTURE DESCRIPTION.	RADIATION COUNT Microcuries (μCi)
N10 23 10.0 E11 41 32.7	Ferruginized and silicified sandstones	1.38×10^{5}
N10 23 08.3 E11 41 31.8	Ferruginized and silicified sandstones	1.85×10^{5}
N10 23 07.4 E11 41 31.3	Ferruginized sandstones	1.59×10^{5}
N10 23 30.0 E 11 42 20	Gneiss	1.85×10^{5}
N10 23 04.8 E11 41 31.8	Sandstones with clay pockets	9.9×10^{4}
N 10 23 20.0 E 11 41 30.0	Ferruginized Sandstones	1.55×10^{5}
N10 22 49.2 E11 41 20.7	Ferruginized sandstones	1.75×10^{5}
N10 22 36.9 E11 41 51.6	Feldspar rich pegmatite dyke (pinkish)	1.31×10^{5}
N10 22 36.9 E11 41 51.6	Granite	1.43×10^{5}
N10 22 34.8 E11 41 50.6	Feldspathic gneiss	2.20×10^{5}
N10 22 43.7 E11 41 53.2	Porphyritic feldspars	1.05×10^{5}
N10 22 30.0 E11 41 39.4	Biotite granite	1.45×10^{5}
N10 22 28.1 E11 41 51.8	Feldspathic gneiss	1.12×10^{5}
N10 22 23.7 E11 41 49.5		1.06×10^{5}
N10 22 20.2 E11 41 45.7	Silicified sandstone + Agate	1.20×10^{5}
N 10 22 15.0 E 11 41 15.8	Silicified Sandstone	1.82×10^{5}
N10 22 10.4 E11 41 43.9	Quartz + Agate	1.79×10^{5}
N10 22 07.6 E11 41 43.2	Agate	1.55×10^{5}
N10 22 06.9 E11 41 43.4	Agate sand	1.20×10^{5}
N10 22 05.8 E11 41 43.1	Agate sand	1.50×10^{5}
N 10 22 10.9 E11 41 49.3	Migmatites	1.50×10^{5}
N 10 22 35.3 E 11 42 15.7	Gneiss	1.45×10^{5}
N10 22 27.8 E11 41 54.1	Biotite granite	7.50×10^{4}
N10 23 23.0 E11 41 53.4	Purple sandstones	1.21×10^{5}
N10 23 01.2 E11 41 45.0	Purple Sandstone	1.55×10^{5}
N10 23 17.8 E11 42 07.2	Purple sandstones	1.82×10^{5}
N 10 23 15.9 E11 42 32.1	Pegmatitic feldspar	1.78×10^{5}
N10 23 19.6 E11 42 36.6	Pegmatite ridge	1.72×10^{5}

COORDINATE	INFERRED ROCK TYPE/STRUCTURE DESCRIPTION.	RADIATION COUNT Microcuries (μCi)
N10 23 22.7 E11 42 38.3	Pegmatite dyke	2.06×10^{5}
N10 23 22.8 E11 42 38.8	Pegmatite dyke	9.90×10^{4}
N10 23 16.7 E11 42 42.6	Pegmatite + Gneiss	1.13×10^{5}
N10 23 32.4 E11 42 43.1	Silicified sandstones	3.55×10^{5}
N10 23 15.0 E11 42 32.9	Quartz pegmatite	1.22×10^{5}
N10 22 21.4 E11 41 42.22	Pegmatite dyke	1.55×10^{5}
N 10 22 30.3 E 11 42 25.6	Gneiss	7.50×10^{4}
N10 22 36.7 E11 41 34.3	Silicified sandstones	1.84×10^{5}
N10 22 35.8 E11 41 35.9	Silicified sandstones	1.88×10^{5}
N10 22 30.0 E11 41 36.9	Feldspathic Granite	6.40×10^{5}
N10 22 23.0 E11 41 39.4	Silicified sandstones	2.52×10^{5}